

INFN-LASA EXPERIMENTAL ACTIVITIES ON PIP-II LOW-BETA CAVITY PROTOTYPES

M. Bertucci*, A. Bosotti, A. D'Ambros, A. T. Grimaldi, P. Michelato,
L. Monaco, C. Pagani¹, R. Paparella, D. Sertore, INFN-LASA, Segrate (MI), Italy
A. Gresele, M. Rizzi, A. Torri, Zanon Research & Innovation, Schio (VI), Italy
¹also at Università degli Studi di Milano, Milano (MI), Italy

Abstract

This paper reports on the first results obtained by INFN-LASA on PIP-II low-beta cavity prototypes. The goal of this activity was to validate the reference surface treatment based on Electropolishing as bulk removal step. The cavity treatment procedures are here presented together with the strategy used for their optimization. The experimental results of cavity cold tests for a single cell prototype are presented and discussed. Having this cavity achieved the requested performance, the baseline procedure is considered as validated and a plan for a future high-Q cavity surface treatment is proposed.

INTRODUCTION

In the framework of the PIP-II international project, INFN-LASA is appointed to build 40 650 MHz $\beta = 0.61$ superconducting cavities that will constitute the low-beta section of the Linac. Specifications for cavity operation in the machine are $E_{acc} = 16.9 \text{ MV m}^{-1}$ with a $Q_0 \geq 2.4 \cdot 10^{10}$. As emerged in the recent past from the series production of ESS 704.4 MHz $\beta = 0.67$ cavities [1], the choice of Buffered Chemical Polishing (BCP) as bulk surface treatment would limit the cavity performance below the PIP-II target value. Basing on this, Electropolishing (EP) was chosen for the upcoming production of PIP-II cavities.

Cavity prototype production is currently ongoing at the firm Zanon Research & Innovation Srl. The EP plant currently in operation is the same used in the past for the treatment of E-XFEL and LCLS-II 1.3 GHz cavities [2]. As already reported in [3], a careful experimental campaign was performed to optimize the EP treatment parameters to the different size and shape of PIP-II cavity. Several short (some tens of μm) EP treatments were done on the single-cell prototype cavity B61S_EZ_002, until the outcome resulted satisfying in terms of surface smoothness, removal rate and iris/equator removal ratio. Being this optimization phase successfully completed, the single cell cavity was ready to undergo the complete baseline treatment, employing a E-XFEL-like recipe [4]. Once the baseline recipe is validated by the results of cavity cold test, the same recipe is expected to be used on a multicell prototype cavity, but with the introduction of a high-Q surface treatment which will allow to reach the PIP-II target.

* michele.bertucci@mi.infn.it

CAVITY SURFACE TREATMENT

The baseline surface treatment employed on the PIP-II single cell prototype cavity B61S_EZ_002 is based on the same recipe used for the series production of EXFEL 1.3 GHz cavities, with the only variation of cold EP as final surface treatment. Cold EP allows to obtain a smoother surface and a more uniform removal over the cavity [5] and is expected to be crucial for the optimization of high-Q treatment recipe. Smoothness is essential for obtaining an high Q-value at the operating gradient, because a rough surface would introduce non-linear losses increasing cavity power dissipation at higher fields [6].

The main steps of the baseline recipe are:

- 150 μm bulk EP, in two separate steps of 75 μm each.
- 800 °C heat treatment for 2 hours in ultra high vacuum (UHV) conditions.
- 25 μm final Cold EP.
- High pressure rinsing (HPR) for 12 hours with ultra pure water (UPW).
- 120 °C 48 h low temperature baking.

After each step, the cavity was HPR-rinsed for 2 hours, weighted and dried. A RF check was repeatedly done so to monitor the frequency response during the treatment steps.

Bulk EP

The bulk EP overall target removal was 150 μm , to be performed in two separate substeps of 75 μm each. The experience gained with the short treatment trials allowed the optimization of treatment parameters and of the plant layout:

- A 30 mm diameter aluminium cathode was employed, with a cylindrical enlargement installed at the equator position, so to locally increase the removal. Fresh acid flows in the cavity through a hole at equator position with a 1 L min^{-1} throughput. The cathode was shielded with a PTFE tape in correspondance of beam tubes.
- A $V = 17 \text{ V}$ voltage was employed, which yielded a 48 A average current and a 0.14 $\mu\text{m min}^{-1}$ removal rate. According to this value, each substep lasted around 10 hours.
- The temperature setpoint of 20-21 °C for the average reading of cavity thermocouples was chosen. When

this value was exceeded, the acid chiller turned on. Moreover, an external water chiller was activated in case of the temperature on beam tube went above 25 °C.

The treatment behavior was monitored online by the instantaneous reading of current and of the several thermocouples installed on cavity surface. The temperature and current readings for the first 100 minutes of the first EP step are shown in Fig. 1. Voltage was turned on at minute 10. Temperatures and current started to rise, consistently with the onset of the electropolishing reaction. Temperature at beam tube quickly rised, going above 25 °C at minute 17 then activating the external water chiller. Then, acid inlet temperature and current started to slowly increase due to the heat generated by the reaction. Temperature setpoint was exceeded around minute 60. Then the acid chiller turned on, driving the process towards an equilibrium condition.

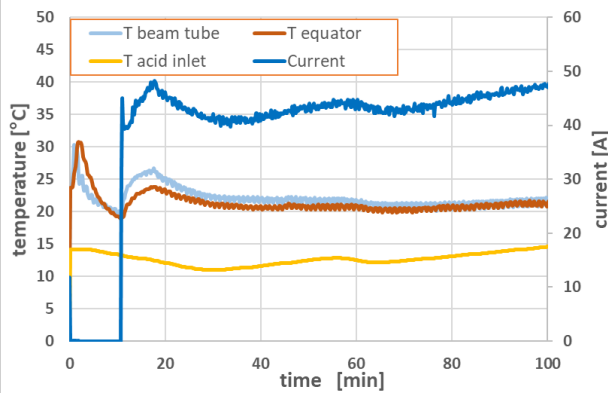


Figure 1: Data from the first 100 min of first EP step: acid inlet, beam tube and equator temperature, and current.

An apparatus allowing continuous acquisition of thickness was purposely developed [7]. This setup allows to connect on cavity surface up to 6 ultrasound transducers and therefore to simultaneously monitor the removal trend in various points of interest. During this treatment, 3 probes were placed on cavity iris, wall and equator, respectively. The whole data registration during the first EP substep is shown in Fig. 2.

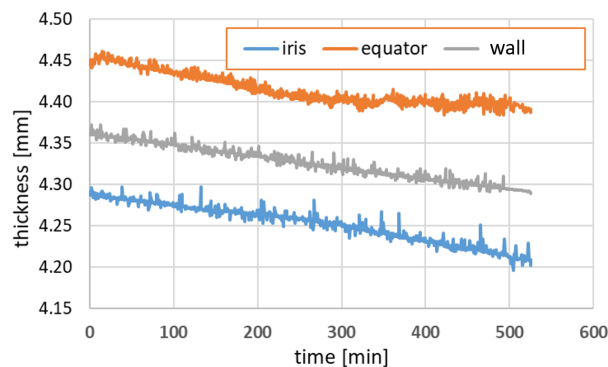


Figure 2: US thickness registration from cavity iris, equator and wall for the first 75 μm EP substep.

The overall removals and removal rates, as extrapolated from the data in Fig. 2, are shown in Table 1. These were consistent with the average values estimated by cavity weighting, which are 157 μm and 0.14 μm min⁻¹. All this considered, and taking also in account the improved surface smoothness at the equator zone as resulted by optical inspection, the EP treatment was considered successful so that the cavity could undergo the following treatment steps.

Table 1: Total Thickness Removal and Removal Rates at Different Points of the Cavity Surface

Step	Removal Parameter	Iris	Wall	Equator
1	rate [μm min ⁻¹]	0.15	0.13	0.12
	removal [μm]	82	71	61
2	rate [μm min ⁻¹]	0.14	0.12	0.11
	removal [μm]	76	70	59

Cold EP

After the 800 °C annealing in a UHV oven, the cavity underwent the final surface treatment. The Cold EP consisted of two separate phases: the first “warm” phase exploited the same treatment parameters of the bulk EP, with a 20-21 °C temperature setpoint for acid inlet chilling. The process lasted until the overall charge removal corresponded to 15 μm average removal on cavity surface. Then, the voltage was turned off and the acid in the barrel was cooled down to 7-8 °C. Once this temperature was reached, voltage was turned on again and the “cold” phase began, with a lower setpoint for acid chilling (max 15 °C on cavity cell, max 18 °C on beam tubes). The process was definitely stopped after an average removal of others 10 μm. The overall temperature and current trend of the cold EP treatment is depicted in Fig. 3. The colder acid temperature produced a significant decrease of current, which dropped from 50 A to around 30 A. In its turn, removal rate went from 0.14 μm min⁻¹ to 0.09 μm min⁻¹, as it expected by the lower temperature which slows down the reaction rate and the diffusion at the niobium surface [8].

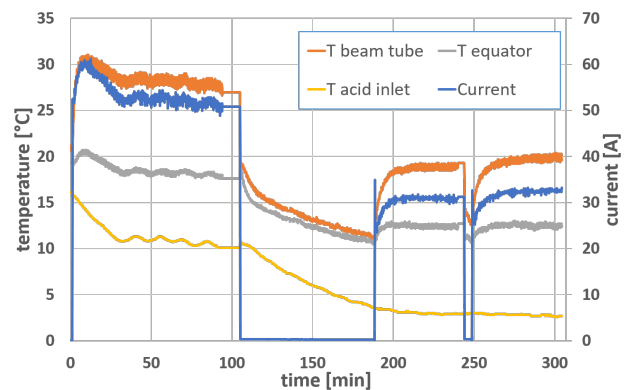


Figure 3: Temperature and current trend during the Cold EP treatment.

CAVITY TEST

After the surface treatment is completed, cavity B61S_EZ_002 was tested at INFN-LASA vertical test facility. The cryostat allows to reach temperatures as low as 1.5 K. The cavity test stand is equipped with diagnostics for the detection of quench events (second sound, fast thermometry) and field emission (photodiodes inside cryostat, external proportional counter and NaI scintillator) [9].

A fluxgate cryogenic sensor was placed on the cavity surface to measure magnetic flux expulsion across the critical temperature (9.2 K). Cooldown rate was less than 1 K min^{-1} so the residual magnetic field (max. 8 mG in the cryostat inner volume) is expected to be completely trapped. Indeed, no magnetic flux variation was measured by the fluxgate. Assuming a trapped flux sensitivity of $0.3 \text{ n}\Omega \text{ mG}^{-1}$ [10] for baked niobium at 650 MHz, one should then expect a $R_{fl} = 2.4 \text{ n}\Omega$ contribution to residual surface resistance.

Cavity surface resistance was measured during the cooldown. Fig. 4 shows the experimental R_s vs T and the data fit performed with SUPERFIT 2.0 code [11], which employs Halbritter quasi-exponential formula for the BCS resistance. The fit results for reduced band gap, electron mean free path and residual resistance are reported in the box inside the graph.

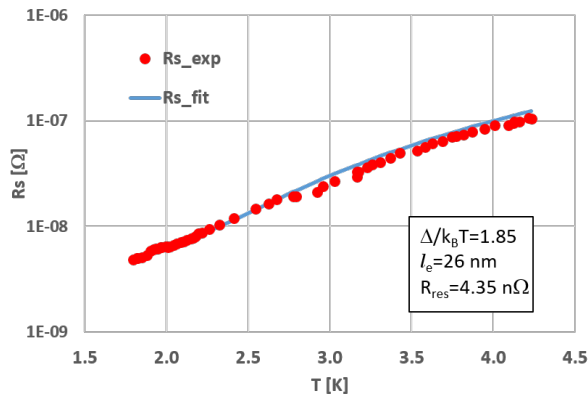


Figure 4: Experimental and fitted R_s vs T curves for cavity B61S_EZ_002.

The results of the vertical tests performed at INFN-LASA lab are shown in Fig. 5. In the first test at 2 K the cavity reached 30 MV m^{-1} , displaying a high-field Q-slope. This behavior is related to field emission, which converts part of the incident power into electron dark current. High-field RF conditioning was attempted so to mitigate the level of field emission. The conditioning was interrupted after 40 minutes due to limitations of the cryogenic plant. The test was then repeated, and a slight degradation of Q_0 at high fields was noticed, together with the increase of radiation level of an order of magnitude. Even the onset of FE displaced from 17 MV m^{-1} to 12 MV m^{-1} . However, radiation level was of the order of $10 \mu\text{Sv h}^{-1}$ near the target gradient of 16.9 MV m^{-1} . This phenomenon is likely to be related to the change in the field enhancement factor of the emitter

during the RF processing session. A longer session would have been beneficial, allowing to reach higher local current densities so to melt permanently the emitter.

From the performance point of view, $Q_0 = 2 \cdot 10^{10}$ at $E_{acc} = 16.9 \text{ MV m}^{-1}$, which corresponds to $R_s = 5.6 \text{ n}\Omega$. It must be stressed that the test was done in a slow cooldown regime so that one can easily get rid of a $R_{fl} = 2.4 \text{ n}\Omega$ contribution to residual resistance by exploiting a proper magnetic hygiene protocol. Assuming a perfect flux expulsion, or canceling the external magnetic field by compensation coils, one can calculate the theoretical Q_0 by subtracting R_{fl} from the experimental surface resistance R_s . Thus, a $Q_0 = \frac{G}{R_s - R_{fl}} = 2.5 \cdot 10^{10}$ can be virtually obtained.

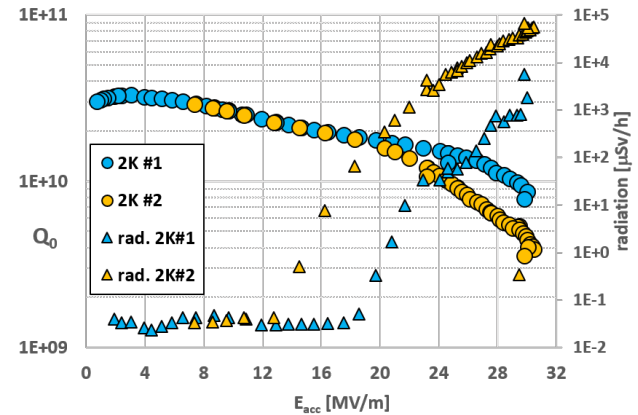


Figure 5: Q_0 vs E_{acc} before and after high-field RF processing. The radiation level is also shown on the secondary axis.

CONCLUSIONS

A 650 MHz $\beta = 0.61$ single cell prototype for PIP-II underwent a complete surface treatment. The main challenge was to obtain good surface smoothness at the end of EP treatment so to prevent non linear losses causing Q-degradation at the target gradient of 16.9 MV m^{-1} . According to the test results, cavity performances are close to the target Q_0 even though a baseline recipe was employed, and in spite of a not optimized magnetic hygiene protocol. As a matter of fact, baseline recipe would be enough to meet the PIP-II specifications assuming no contribution of external magnetic field to surface resistance. Field emission can be of some concern, although the radiation level at the target gradient was low and several strategies of mitigation are nowadays available [12].

Given this, we considered the baseline treatment of the single cell cavity validated. The experience so far gained is at the basis of the high-Q surface of treatment of a prototype multicell cavity, which is planned for the next future.

REFERENCES

- [1] A. Bosotti *et al.*, "Vertical Tests of ESS Medium Beta Prototype Cavities at LASA", in *Proc. 8th Int. Particle Accelerator Conf. (IPAC'17)*, Copenhagen, Denmark, May 2017, pp. 1015–1018. doi:10.18429/JACoW-IPAC2017-MOPVA063

- [2] M. Rizzi, G. Corniani, A. Matheisen, and P. Michelato, “Comments on Electropolishing at Ettore Zanon SpA at the End of EXFEL Production”, in *Proc. 17th Int. Conf. RF Superconductivity (SRF’15)*, Whistler, Canada, Sep. 2015, paper MOPB102, pp. 394–398.
- [3] M. Bertucci *et al.*, “Electropolishing of PIP-II Low Beta Cavity Prototypes”, in *Proc. 19th Int. Conf. RF Superconductivity (SRF’19)*, Dresden, Germany, Jun.-Jul. 2019, paper MOP057, pp. 194–198.
- [4] W. Singer *et al.*, “Production of superconducting 1.3-GHz cavities for the European X-ray Free Electron Laser”, *Physical Review Accelerators and Beams*, vol. 19, no. 9, p. 092001, Sep. 2016.
doi:10.1103/PhysRevAccelBeams.19.092001
- [5] F. Furuta, D. Bice, A. C. Crawford, and T. Ring, “Fermilab EP Facility Improvement”, in *Proc. 19th Int. Conf. RF Superconductivity (SRF’19)*, Dresden, Germany, Jun.-Jul. 2019, paper TUP022, pp. 453–455.
- [6] K. Saito, “Surface Smoothness for High Gradient Niobium SC RF Cavities”, in *Proc. 11th Workshop RF Superconductivity (SRF’03)*, Lübeck, Germany, Sep. 2003, paper THP15, pp. 637–640.
- [7] M. Bertucci *et al.*, “An apparatus for the continuous measurement of thickness during the electropolishing of superconducting cavities”, *Review of Scientific Instruments*, vol. 92, no. 2, p. 023307, Feb. 2021. doi:10.1063/5.0028778
- [8] C. Reece, “An Experimental Analysis of Effective EP Parameters for Low-Frequency Cylindrical Nb Cavities”, in *Proc. 19th Int. Conf. RF Superconductivity (SRF’19)*, Dresden, Germany, Jun.-Jul. 2019, paper TUP029, pp. 472–476.
- [9] M. Bertucci *et al.*, “Quench and Field Emission Diagnostics for the ESS Medium-Beta Prototypes Vertical Tests at LASA”, in *Proc. 8th Int. Particle Accelerator Conf. (IPAC’17)*, Copenhagen, Denmark, May 2017, pp. 1007–1010.
doi:10.18429/JACoW-IPAC2017-MOPVA061
- [10] M. Checchin *et al.*, “Frequency Dependence of the Trapped Flux Sensitivity in SRF Cavities”, *Applied Physics Letters*, vol. 112, no. 7, p. 072601, Feb. 2018.
doi:10.1063/1.5016525
- [11] G. Ciovati, “SUPERFIT: a Computer Code to fit Surface Resistance and Penetration Depth of a Superconductor”, Thomas Jefferson National Accelerator Facility (TJNAF), Newport News, VA, USA, Rep. JLAB-ACC-03-226, Jan. 2003.
- [12] B. Giaccone *et al.*, “Field emission mitigation studies in the SLAC Linac Coherent Light Source II superconducting rf cavities via in situ plasma processing”, *Physical Review Accelerators and Beams*, vol. 24, no. 2, p. 022002, Feb. 2021.
doi:10.1103/PhysRevAccelBeams.24.022002